

**A semi-automated technique for repeatable and reproducible contact angle
measurements in granular materials using the Sessile Drop Method**

Y. Saulick ^{a*}, S.D.N. Lourenço ^a, B.A. Baudet ^b

^a Department of Civil Engineering, Haking Wong Building, The University of Hong Kong,
Pokfulam Road, Hong Kong SAR

*Corresponding author (yunesh@connect.hku.hk)

^b Department of Civil, Environmental and Geomatic Engineering, University College,
London, Gower Street, London WC1E 6BT, UK; formerly The University of Hong Kong

ABSTRACT

Contact angles (CAs) are used to measure the extent to which a material is wettable. Granular materials such as natural soils and crushed minerals, which are commonly assumed wettable, can exhibit non-wetting characteristics. The sessile drop method (SDM) is a direct method widely used to generate and measure CAs, however, the procedure involved in their determination is often overlooked leading to very large standard deviations in their measurements. In this study, a close examination of the steps involved in extracting the CAs on granular materials shows that two factors, the image exposure and the position of the baseline, can affect CAs measurements significantly. Seven methods of fitting contact angles were compared. It was found that the discrepancy between the methods became more and more significant as CAs increase in magnitude. A semi-automated technique has therefore been proposed through this study to improve the standard deviations of CAs measurements. The new technique uses five steps and involves an adjustment of the image exposure and manual movement of the baseline. The proposed method was tested on flat surfaces as well as granular materials (chemically treated sand and a naturally occurring hydrophobic mineral). The results have shown that the method can be applied for both flat and granular materials with a wide range of CAs. In particular, the standard deviations of flat surfaces (e.g. hydrophobised microscope slides) with CA in the range of 90° - 135° , improvements of 37% have been recorded. For granular materials (e.g. fluorspar) with CA in the range of 105° - 120° , improvements of 33% in standard deviations have been observed.

LIST OF ABBREVIATIONS

CA: Contact Angle

CD-R: Compact Disk

DSA: Drop Shape Analyser 25

LBS: Leighton Buzzard Sand

LBADSA: Low-Bond Axisymmetric Drop Shape Analysis

RSI: Relative Sharpness Index

SDM: Sessile Drop Method

1.0 INTRODUCTION

The wetting properties of natural and synthetic materials are usually assessed by means of the contact angle (CA). The simplest and most straightforward way of determining the CA is to measure it directly on the substrate. The sessile drop method (SDM) makes a direct measurement of the CA at the solid-liquid-vapour phase of the boundary and thus quantifies the extent to which a soil is wettable (Adamson, 1990). Alternative methods to obtain the CA include the Wilhelmy plate method, captive bubble method, thin column wicking method, capillary rise and modified capillary rise method. The Wilhelmy plate method (as used in Ramires-Flores *et al.*, 2010) yields two dynamic CAs (the receding and advancing CAs). In their study to investigate the wettability of minerals, Lourenço *et al.* (2015b) used the advancing CA as a measure of wettability. A disadvantage of the method is that since the sample is immersed into a liquid (usually water), the sample may react or swell. The captive bubble method as used in Pogorzelski *et al.* (2013) is also susceptible to such drawbacks.

As opposed to CAs measured using the capillary rise method (as used in Letey *et al.*, 1962; Bachmann *et al.*, 2000b), where the range of measurements is restricted to $< 90^\circ$, CAs measured with the SDM vary within the range 0° (for very wettable surfaces) to 180° (for non-wettable surfaces). Moreover, for techniques such as the capillary rise method

and thin column wicking method (as used in Hajnos *et al.* 2013), the use of a soil column makes it difficult to control the resulting soil structure and fabric which influence the resulting CA. Similar issues also arise when the modified capillary rise method (as used in Bachmann *et al.*, 2003) is used to generate CAs measurements. As with the aforementioned techniques, the methods of preparing samples for measurement using the SDM highly influence the resulting CA. In fact, the precision of such a measurement requires the drops to be placed on homogeneous and plain surfaces (Drelich, 1997). In previous studies of water repellent sands conducted by Bond (1968), the ‘flattened surface of a sample’ was used without explicitly describing how this was achieved. Chassin *et al.* (1986) and subsequently Valat *et al.* (1991) tried to replicate flat surfaces by placing their samples into disks and applying pressure on them. They however used relatively compressible materials such as clay montmorillonite, peat and compost materials for which flat surfaces can be more easily achieved than in sandy soil. Due to their relatively low compressibility compared to clays and peats, sandy soils offer a rough surface, which significantly impede the measurement of CA by the SDM.

Bachmann *et al.* (2000a) followed a similar method applied to sandy materials, which have initially been air-dried. By making use of different sieved fractions, Bachmann *et al.*

(2000a) showed that it was possible to limit heterogeneous regions and thus approximate the surface produced by granular materials to a flat one. They placed a double-sided tape on a smooth microscope glass slide prior to sprinkling the soil particles on it which is probably different to what Bond (1968) did. The main purpose of the tape is to prevent any motion of the particles when the liquid is deposited on the substrate. Bachmann *et al.* (2000b) later showed in a study investigating the effect of increasing the percentage of wettable particles on the apparent CA, that the trend observed with and without the tape was similar, i.e. an increase in the proportion of wettable particles decreased the CA. The resulting lump of material produced is then lightly pressed, followed by gently shaking the excess material. These steps are carried out twice and in so doing, ensure that the area offered by the tape is covered as much as possible.

The CA is then measured using a goniometer (Figure 1). A syringe is used to dispense a pre-determined volume of liquid on the substrate. The drop of liquid, referred to as a sessile drop, is subjected to a light source on one side of the device with the magnifying lens within the camera on the other side able to capture a series of images, which are then displayed on a computer screen. The main reason for recording a series of images is to be able to eventually select that image which corresponds to the immediate impact of the

drop of the liquid with the substrate. This is because the longer the drop is in contact with the substrate, the more infiltration there will be in the case of porous materials such as soil or, in the case of flat surfaces, the more spread the drop will be. Once the image is acquired, the drop shape is fitted to obtain the CA. Despite using software to improve the fitting, thus reducing subjectivity associated with operator's usage to some extent, there are several factors, which influence the measurement of CAs from the moment the image is initially captured to its eventual processing. While researchers limit observational errors as much as possible, the intrinsic heterogeneity of the materials being analysed as well as the absence of a methodological approach contribute to the relatively large standard deviations encountered in some studies (Table 1). The table shows that standard deviations as high as $\pm 25^\circ$ has been observed in Lourenço *et al.* (2015a). Relatively smaller values such as $\pm 6^\circ$ (Leelamanie & Karube, 2012) are not uncommon. While the standard deviations in CAs measurements reported in the early 2000s may be ascribed to the lack of sophisticated equipment available at the time, it is interesting to note that in spite of the advent of CCD-equipped goniometers, there have been little improvements in the standard deviations. In many cases, the steps involved once an image is obtained from a goniometer are abstruse which therefore questions both the 'repeatability' and the 'reproducibility' of the measurements. The term 'repeatability' refers to CAs

measurements carried out with the same material, apparatus, environmental conditions, operator with measurements performed in the shortest time and the term ‘reproducibility’ relates to the same material but different operator, apparatus and in certain cases different environmental conditions (TAPPI, 2000). Although obtaining repeatable and reproducible CAs with a methodological approach is crucial for experimentalists, it should be emphasised that data, which shows repeatability as well as reproducibility, are not synonymous to exact and absolute values.

In this paper, the main causes of large discrepancy amongst CA data were identified. A semi-automated technique was then developed to reduce the standard deviations of CAs and to ensure their repeatability and reproducibility in both flat and granular materials at a wide range of CAs.

2.0 MATERIALS AND TESTING PROCEDURES

2.1 MATERIALS

Both flat and granular surfaces were tested. For the granular surfaces, Leighton Buzzard Sand (LBS), a quartzitic sand available from the UK was used. Four different sieve fractions were chosen (< 0.3 mm, 0.3 – 0.425 mm, 0.425 – 0.6 mm and 0.6 – 1.18 mm) and each was air-dried (water content = 0.25%) before changing its wettability. To alter

the wettability of the LBS samples, dimethyldichlorosilane, a hydrophobising agent usually added to soil samples (e.g. Goebel *et al.*, 2007; Ng & Lourenço, 2016) was used. This silane compound was added by means of a pipette capable of gauging up to one microlitre. This was followed by gentle stirring of the soil for a couple of minutes in a fume hood until no hydrogen chloride fumes were produced. The samples were then sealed in plastic bags for 24 hours prior to any measurement. In addition to the chemically modified LBS, fluorspar, a naturally hydrophobic mineral was tested. The mineral, initially of size 1cm was washed with de-ionized water and allowed to dry at a temperature of 30°C before being crushed in a jaw-crusher (reduced to gravel-size materials) and then grinded in a ball mill. The resulting fluorspar particles were then sieved and particles in the range of 0.212-0.425 mm were isolated for eventual analyses.

The flat surfaces used were microscope glass slides with dimensions 76 by 26 mm, thicknesses of 1 mm (made of soda-lime-silica glass obtained from Isolab Laborgeräte GmbH) and a compact disc (Brand: Philips, Type: CD-R, Maximum Storage Capacity: 700MB/80min, Maximum Writing Speed: 52x, Diameter: 12cm). These materials were selected because in addition to offering a flat surface, they also provide good reflectivity once a liquid is in contact with them. Besides these two characteristics, the CD-R,

composed primarily of a polycarbonate plastic is likely to exhibit different wetting behaviour as opposed to the silica-made microscope glass slides.

2.2 CA MEASUREMENTS

A survey carried out on a series of goniometers from different manufacturers (DataPhysics corporation, First Ten Angstroms Incorporation and ramé-hart instrument company) has shown that goniometers essentially possess the same hardware components and undergo similar image analysis procedures. The measurements of CA are therefore not apparatus-dependent but rather user-dependent. The goniometer used in the study is the Drop Shape Analyser 25 (DSA) from KRÜSS GmbH. The device consists of the following hardware components: standard dosing unit, standard sample table PS4000 and a CCD camera 1394 AVT, all linked to a desktop computer. The image captured by the camera is a greyscale image (also called an 8-bit image) where the extreme pixel intensity values of 0 and 255 correspond to the black and white colours respectively which is then analysed by the software incorporated in the DSA (version 1.92.1.1). The resulting data extracted from these images are therefore influenced by the outline of a particular surface, which is represented by different intensities of grey colours.

All measurements of CAs were carried out using a 10 μl drop of de-ionized water initially passing through a glass syringe (maximum capacity of 500 μl) and eventually being dispensed by a needle (Material: Steel, Diameter: 0.513 mm and Length: 38 mm from the NE94 assortment by KRÜSS GmbH). This volume was chosen as it was established that this was the minimum volume, which could be provided by the needle that would allow the drop to initiate contact with the substrate rather than hang from the needle. The DSA allows control over the dosage rate at which the drop is dispensed and in this study, a dosage rate of 100 $\mu\text{l}/\text{min}$ was opted for, because at higher values, the vibration caused by the DSA upon dispensing the liquid affected both the volume dispensed and the time needed to extract the frame to be analysed. The motion of the drop from the needle to the substrate was recorded by the CCD camera (83 frames per second) and in accordance with the studies carried out by Shang *et al.* (2008) and Bachmann *et al.* (2013), the initial CA was considered to be the most representative measure of wettability. It takes on average 6 seconds for the drop to be dispensed and leave the tip of the syringe to reach the substrate. However, an additional 50 ms is required upon contact with the substrate so that the image obtained is not blurry. This corresponds to 3-4 frames. CA measurements on the granular materials were prepared according to the technique proposed by Bachmann *et al.*, (2000a) by fixing a monolayer of particles on a microscope slide with double-sided tape

attached to it. However, because the fluorspar particles were more angular than the LBS particles, the resulting layer and the packing between the particles were different. This factor could have influenced the absolute value of CA measurements. All measurements were carried out under controlled laboratory conditions at a temperature and relative humidity of 23 ± 2 °C and 55 ± 5 % respectively.

3.0 RESULTS AND DISCUSSION

3.1 OPTIMISATION OF IMAGE

The acquisition of images can be optimised by making concurrent use of the optics settings and the DSA software. The zooming and focussing options are controlled by two rotating rings incorporated in the camera used for magnification, and enhance the sharpness of the image. The exposure of the image, which is a representation of its quality is dictated by the amount of light and the time to which the image sensor in the camera is subjected to the light source. The quantifiable and adjustable parameters provided by the DSA program, which control exposure are illumination, shutter speed and signal gain. They are elaborated in the following sub-sections.

3.1.1 ILLUMINATION, SHUTTER SPEED AND SIGNAL GAIN

The illumination (adjusted on a scale of 0 to 100) referred to as ISO in digital photography parlance is a measure of how sensitive the image sensor of the camera is to light. The larger the illumination (values close to 100), the more sensitive the image sensor is. To obtain the finest image, there should be a contrast between the drop of liquid and the background.

The shutter speed (adjusted on a scale of 1 to 4095) controls the amount of time that light strikes the image sensor. While a fast shutter speed (values close to 4095) might be able to record the movement of a drop falling from the syringe to a surface perfectly, the image obtained might not be bright enough for an eventual analysis since only a small lapse of time is allowed for the light to hit the image sensor.

The signal gain (adjusted on a scale of 0 to 680) is an electronic intensification or curtailment of the electric signal from the sensor used to brighten the image in the absence of adequate light. However, increasing the signal gain produces a brighter image at the expense of clarity.

3.1.2 GAUGING THE EXPOSURE OF THE IMAGE USING THE SURFACE TENSION OF DE-IONIZED WATER

The software integrated in the DSA offers a useful tool termed as ‘focussing assistant’ to guide users gauge the exposure by means of a median relative sharpness index (RSI). The RSI can therefore be considered as an indication of the exposure of the image. The larger this number is, the more suitable the image is for analysis. The RSI is sensitive to small changes in the illumination, shutter speed or signal gain and isolating any one of them and increasing/decreasing its value only will not lead to a better exposure. A combination of illumination, shutter speed and signal gain leading to a large RSI value is therefore important.

The relevance of the RSI in the adequate identification of the silhouette of a drop is shown via a parametric study where the surface tension of de-ionized water was measured using the DSA by analysing a pendant drop (Figure 2). The diameter of the steel needle and the volume of the pendant drop were 1.852 mm and 30 μ l respectively. The adequacy of the RSI was determined by the fit errors generated by the DSA software and the absolute value of surface tension of de-ionized water. In this exercise, the RSI was varied by changing the illumination, shutter speed and signal gain to alter the quality of the image and thus its RSI.

The effect of the RSI on the fit errors is illustrated in Figure 3. As the RSI decreases from the range >120 to 40-50, the fit errors increase from 1.70 μm to 5.72 μm . The drop in RSI is also accompanied by significant deviations from the typical values of surface tension of water, which usually do not exceed 74 mN/m for temperatures varying between 15 °C to 25 °C (Vargaftik *et al.*, 1983). A change in surface tension from 74.32 mN/m to 78.24 mN/m was observed as the RSI switched from >120 to 40-50. Taking into consideration the limitations in adjusting the RSI, a threshold minimum RSI value of 70 was deemed suitable for adequate measurement using the DSA. All measurements using the DSA which follows have been carried out with RSI values ≥ 70 .

3.2 METHODS OF FITTING DROP PROFILES FOR CA MEASUREMENTS WITH OPTIMISED IMAGES

3.2.1 FITTING METHODS

The DSA offers at least four automated techniques for the evaluation of CAs amongst which are the *Tangent-1*, *Tangent-2*, *Circle* and *Laplace-Young*. A brief description of how these mathematical approximations (referred to as fitting methods) are carried out is shown in Table 2.

In addition to the automated fitting methods provided by the DSA, users can also export the extracted pictures to image processing packages for eventual analysis. One of them is

the open source and multi-platform image-processing package, Image J (available at: <http://imagej.nih.gov/ij/>). It offers three additional fitting methods. One of them is an in-built function within the software called *Angle Tool* and the other two are known as the *DropSnake* and *Low-Bond Axisymmetric Drop Shape Analysis, LBADSA*. The former is a fully manual tool and requires the operator to identify the three-phase contact point. *DropSnake* allows a user to manually define parts of the contour of the sessile drop, after which, a piecewise continuous curve is used (similar to a polynomial fitting). *LBADSA* uses the sessile drop image and fit it with a solution of the Young-Laplace equation (Stalder *et al.*, 2010). Analysis using the latter method makes use of the whole drop profile. A full description on the usage and optimisation of the *DropSnake* and *LBADSA* is provided in Stalder *et al.* (2010; 2006).

3.2.2 BASELINE POSITION

Besides the identification of the outline of the profile and its fitting, the baseline and its position also form part of the evaluation of the CA by the SDM. Woodward (1999) in his study of flat surfaces mentions that the error associated in identifying the baseline in a sessile drop measurement is the major reason for inaccurate CA measurements. To circumvent this problem, the same author recommends setting the camera at a suitable angle (around 2-3°) prior to measurement so that the baseline may be identified easily.

While this alternative helps in identifying the baseline on a material which offers a mirror image such as a microscope slide, this is not the case with granular materials such as soil. Figure 4 illustrates the difficulty in identifying the baseline with a sample of hydrophobised LBS. The same figure also shows the extent through which the position of the baseline may vary via a parameter termed as band thickness, B .

The four different sieve fractions of LBS were used to illustrate how B varies with the particle size. The results are shown in Figure 5. The figure demonstrates that an increase in particle size from 0.3 mm up to 1.18 mm increases the value of B by more than 100%, making the identification of the baseline even more difficult and operator-dependent.

The effect of shifting the baseline was tested on the four automated techniques provided by the DSA. The CA of two microscope slides, one of which was hydrophobised was determined by shifting the baseline 0.1 mm above and below the mirror image which should indicate the most likely location of the exact baseline. The values obtained are given in Table 3. Table 3 shows that neglecting the peculiar value obtained from *Tangent-1* (55°), the CA may vary within the range of 9 to 23 % as a result of a change in baseline position by 0.1 mm on a relatively hydrophilic material. For the hydrophobised

microscope slide, this variation may reach 41%, highlighting the significant errors, which may be induced during the CA measurement of hydrophobic samples. A shift in the baseline by 0.1 mm below the mirror image overestimates the CA while a movement of 0.1 mm above the mirror image underestimates the CA. These results further demonstrate that the position of the baseline is important in measuring the CAs of granular materials.

3.2.3 ANALYSIS OF FITTING METHODS

A comprehensive study of how the fitting methods fare on materials with different surface properties seems judicious. Five materials with different chemistry were chosen in this study; two microscope slides (one of which was treated with dimethyldichlorosilane), the CD-R and LBS (sieve fraction <0.3 mm) hydrophobised to two different extents (LBS1 and LBS2). Figure 6 illustrates the results of this investigation after calculating the mean of 10 CAs on each material.

For the microscope slide and LBS1, the *Tangent-1* seems to give a larger value as compared to the other methods. With the microscope slide, the fitting method implemented does not seem to yield large differences in the magnitude of the CAs. The standard deviations between all the techniques of measurements are 3.90° for the microscope slide and 8.90° for LBS1. This increase is mainly because of the lack of

reflection on the surface in the measurement of LBS1 as compared to the microscope slide, which makes it difficult to identify the baseline and also because of fit errors.

With the remaining three materials, namely hydrophobised microscope slide, CD-R and LBS2, the difference in CAs is more significant. The standard deviations between all the techniques of measurements are respectively 13.8°, 12.8° and 14.7°. These values show that discrepancies are more likely to occur with hydrophobic and granular materials. This last observation is further substantiated by an analysis of the fit errors, which are provided only by the automated techniques. In an analogous way to how the threshold value for the RSI was obtained, the fit error in the measurement of CA represents the difference in the fitting method and the extracted profile. Figure 7 demonstrates the use of one of the automated techniques, the *Tangent-2* on a microscope slide. In this case, the presence of the mirror image beneath the drop facilitates the positioning of the baseline. From the same figure, it can be seen that the fitting is carried out on both sides of the drop with the extracted profile (red line) overlaid by the fitting (green line). The fit errors, which depend on the fitting techniques adopted and are in the range of micrometres, have been used to analyse the respective automated techniques. These data are illustrated in Figure 8.

With the three flat surfaces, the *Tangent-1* and *Circle* have their fit errors increasing when the material under consideration is more hydrophobic. For the CD-R, there is a difference in fit error of around 700% with the microscope slide when the *Circle* is used. As for the *Tangent-2* and *Laplace-Young*, the fit errors are very close to each other (the standard deviations of errors are 1.94 μm and 2.23 μm respectively).

For the LBS1 and LBS2, the fit errors are generally larger than the remaining materials regardless of the fitting method adopted. With the *Tangent-1*, the fit error with LBS1 is as high as 114.3 μm (as compared to 5.50 μm for the microscope slide). These results not only suggest that it is more difficult to extract the drop profiles of hydrophobic materials, but also that the automated techniques are adequate only on flat hydrophilic surfaces which allows a clear reflection of drops to be made.

This section has shown that discrepancies between techniques when measuring CA for hydrophobic materials are relatively larger. Compared to the flat surfaces, the fit errors associated with the granular materials have been shown to be larger. This is mainly due to the heterogeneity of the granular materials. In addition, the identification of the baseline for granular materials becomes more difficult when particle size increases. Therefore, to

ensure reliable measurements of CA on materials, which exhibit hydrophobic behaviour, a technique, which takes into consideration these factors, is essential.

3.3 PROPOSED SEMI-AUTOMATED TECHNIQUE FOR CA MEASUREMENTS

The exposure of the image as well as the position of the baseline has been shown to be crucial factors in determining the CAs. Nevertheless, all the measurement techniques described previously (*Tangent-1*, *Tangent-2*, *Circle*, *Laplace-Young*, *Angle Tool*, *Drop Snake* and *LBADSA*) either do not explicitly make use of these factors or are not mentioned. In the case of the exposure of the image, qualitative descriptions have very often been used (e.g. Beatty & Smith, 2010) and for the baseline and its position, the automated methods define an arbitrary baseline from which the CA is eventually generated. In order to restrict the amount of subjectivity regarding the positioning of the baseline, some image processing technique is necessary. As a result, the techniques offered by ImageJ, which allows more versatility towards image manipulations were preferred to the automated techniques. Amongst the three methods introduced earlier, only the *LBADSA* and the *Angle Tool* methods offer flexibility in positioning the baseline. Because the latter is heavily reliant on the operator to determine the three-phase contact point on an image, the *LBADSA* method was implemented and modified as follows:

Step 1: Obtain image from goniometer after adjusting RSI to ≥ 70 .

Step 2: Fitting of drop profile by *LBADSA* method as per the recommendations of Stalder *et al.* (2010).

Step 3: Binarisation of the image, i.e. conversion of the 8-bit image to black and white colours (corresponding to pixel values of 0 and 255 respectively).

Step 4: Generation of outlines of drop and surface.

Step 5: Positioning the baseline as a horizontal tangent to the outline when moving upwards towards drop profile

The above sequence is illustrated in Figure 9 on a sample of LBS (size <0.3 mm). Step 1 of the procedure involves the adjustment of the image exposure and Step 2 refers to the fitting of the whole drop profile. Steps 3 to 5 are carried out for the positioning of the baseline and therefore, the proposed method is not a fully automated one. This new technique termed *Semi-automated* is compared to the existing techniques in terms of standard deviations in CA measurements. The materials tested were microscope slide, hydrophobised microscope slide, CD-R, LBS1, LBS2 and flourspar. Ten CA measurements were carried out on each of these materials and their standard deviations calculated. The results are shown in Figure 10. It can be seen that the *Semi-automated*

technique gives the lowest standard deviations for all the materials considered. For the flat surfaces, besides the *Tangent-1* for the microscope slide and the *Laplace-Young* for the hydrophobised microscope slide and the CD-R, all the techniques give relatively low standard deviations (less than 6°). However, with the granular materials, there is an increase in standard deviations with all the techniques (up to 9° for LBS1). This increase is even more pronounced with the hydrophobised LBS and fluorspar where a standard deviation as high as 17° is observed.

To assess the contribution and enhancement made by the *Semi-automated* technique, its standard deviation was compared to the smallest value amongst the other techniques. For hydrophilic and hydrophobic flat surfaces, the percentage improvement by the *Semi-automated* technique was 2.1% and 37.3% respectively. As for granular materials, the enhancement was 7.4% and 32.9% for the hydrophilic and hydrophobic materials respectively. Since a manual adjustment of the baseline is carried out (step 5) when the *Semi-automated* technique is followed, it is expected that the absolute CAs of the materials under investigation shift in 'one direction' i.e. all measurements performed using the protocol will possess a systematic error. However, because the absolute values of any of the materials investigated are unknown, the magnitudes of the systematic errors

and whether the *Semi-automated* technique yields an over or under estimated value cannot be ascertained.

4.0 CONCLUSIONS

The adequate determination of CA is important in fields such as geotechnical engineering, soil science and mineral engineering where granular materials that are not completely wettable are encountered. A number of studies have revealed large values of standard deviations for the CAs (measured by the SDM or otherwise). In addition, the exact approach and the stepwise methodology adopted in the measurement of CAs by the SDM in the aforementioned disciplines are rarely defined. In this research, it was shown that a modification of a well-established method, which has been developed primarily to measure CAs on flat and reflective surfaces, can yield practical values of CAs on both flat and granular materials. For hydrophobic surfaces, the *Semi-automated* technique developed improves the standard deviation of measurements of CA by 37% and 33% on flat and granular surfaces respectively. With more and more studies focussing on hydrophobic soils as well as flat surfaces and other research aiming at switching originally wettable granular/flat materials to hydrophobic ones, the need for a reliable comparison of CAs will be ever more central.

ACKNOWLEDGEMENTS

This research work has been possible through the funding support provided by The University of Hong Kong. Help and comments by Mr. Shuang Zheng as well as laboratory support from Mr. N.C. Poon are much appreciated.

REFERENCES

ADAMSON, A. W. 1990. Physical chemistry of surfaces, Wiley.

BACHMANN, J., ELLIES, A. & HARTGE, K. 2000. Development and application of a new sessile drop contact angle method to assess soil water repellency. *Journal of Hydrology*, 231, 66-75.

BACHMANN, J., GOEBEL, M.-O. & WOCHE, S. K. 2013. Small-scale contact angle mapping on undisturbed soil surfaces. *Journal of Hydrology and Hydromechanics*, 61, 3-8.

BACHMANN, J., HORTON, R., VAN DER PLOEG, R. R. & WOCHE, S. 2000. Modified sessile drop method for assessing initial soil-water contact angle of sandy soil. *Soil Science Society of America Journal*, 64, 564-567.

BACHMANN, J., WOCHE, S. K., GOEBEL, M. O., KIRKHAM, M. B. & HORTON, R. 2003. Extended methodology for determining wetting properties of porous media. *Water Resources Research*, 39.

BEATTY, S. M. & SMITH, J. E. 2010. Fractional wettability and contact angle dynamics in burned water repellent soils. *Journal of Hydrology*, 391, 99-110.

BOND, R. 1968. Water repellent sands. 9th Trans. Int. Congr. Soil Sci.[Adelaide, Australia], 1, 339-347.

CHASSIN, P., JOUNAY, C. & QUIQUAMPOIX, H. 1986. MEASUREMENT OF THE SURFACE FREE-ENERGY OF CALCIUM-MONTMORILLONITE. *Clay Minerals*, 21, 899-907.

Dataphysics.de. (2016). DataPhysics - OCA measuring instruments. [Online] Available at: <http://www.dataphysics.de/2/start/products/contact-angle-measuring-and-contour-analysis-systems/oca-measuring-instruments/> [Accessed 7 September 2016].

DRELICH, J. 1997. Static contact angles for liquids at heterogeneous rigid solid surfaces. *Polish Journal of Chemistry*, 71, 525-549.

Firsttenangstroms.com. (2016). *Contact Angle and Surface Tension Instruments*. [Online]

Available at: <http://www.firsttenangstroms.com/products/products.html> [Accessed 7

September 2016].

GOEBEL, M.-O., WOCHE, S. K., BACHMANN, J., LAMPARTER, A. & FISCHER, W.

R. 2007. Significance of wettability-induced changes in microscopic water distribution for

soil organic matter decomposition. *Soil Science Society of America Journal*, 71,

1593-1599.

GOEBEL, M. O., BACHMANN, J., REICHSTEIN, M., JANSSENS, I. A. &

GUGGENBERGER, G. 2011. Soil water repellency and its implications for organic

matter decomposition—is there a link to extreme climatic events? *Global Change Biology*,

17, 2640-2656.

HAJNOS, M., CALKA, A. & JOZEFACIUK, G. 2013. Wettability of mineral soils.

Geoderma, 206, 63-69.

KOC, M. & BULUT, R. 2013. Assessment of a sessile drop device and a new testing approach measuring contact angles on aggregates and asphalt binders. *Journal of Materials in Civil Engineering*, 26, 391-398.

KRÜSS 2004-2013. DSA4 Software for Drop Shape Analysis User manual part 2: Working in expert mode, DSA mapping editor, theory V2.0-02, Hamburg, KRÜSS GmbH.

KRÜSS 2004-2014. DSA4 Software for Drop Shape Analysis User manual part 1: Installation, introduction, working in standard mode V2.0-02, Hamburg, KRÜSS GmbH.

LEELAMANIE, D. A. L. & KARUBE, J. 2012. Drop size dependence of soil-water contact angle in relation to the droplet geometry and line tension. *Soil science and plant nutrition*, 58, 675-683.

LETEY, J., OSBORN, J. & PELISHEK, R. E. 1962. Measurement of liquid-solid contact angles in soil and sand. *Soil Science*, 93, 149-153.

LOURENÇO, S., WOCHE, S., BACHMANN, J. & SAULICK, Y. 2015. Wettability of crushed air-dried minerals. *Géotechnique Letters*, 5, 173-177.

LOURENÇO, S. D. N., JONES, N., MORLEY, C., DOERR, S. H. & BRYANT, R. 2015. Hysteresis in the Soil Water Retention of a Sand-Clay Mixture with Contact Angles Lower than Ninety Degrees. *Vadose Zone Journal*, 14.

NG, S. H. Y. & LOURENÇO, S. D. N. 2016. Conditions to induce water repellency in soils with dimethyldichlorosilane. *Géotechnique*, 66, 441-444.

POGORZELSKI, S., MAZUREK, A. & SZCZEPANSKA, A. 2013. In-situ surface wettability parameters of submerged in brackish water surfaces derived from captive bubble contact angle studies as indicators of surface condition level. *Journal of Marine Systems*, 119, 50-60.

Ramehart.com. *ramé-hart Contact Angle Goniometers*. [Online] Available at: <http://www.ramehart.com/goniometer.htm> [Accessed 7 September 2016].

RAMÍREZ-FLORES, J. C., BACHMANN, J. & MARMUR, A. 2010. Direct determination of contact angles of model soils in comparison with wettability characterization by capillary rise. *Journal of Hydrology*, 382, 10-19.

RASBAND, W. S. 1997-2016. *ImageJ*. <http://rsbweb.nih.gov/ij/>. 1.46 ed. Bethesda, MD, USA: US National Institutes of Health.

SHANG, J., FLURY, M., HARSH, J. B. & ZOLLARS, R. L. 2008. Comparison of different methods to measure contact angles of soil colloids. *Journal of Colloid and Interface Science*, 328, 299-307.

STALDER, A. F. Drop Shape Analysis—Free Software for High Precision Contact Angle Measurement [Online]. École Polytechnique Fédérale de Lausanne: Biomedical Imaging Group of École Polytechnique Fédérale de Lausanne. Available: <http://bigwww.epfl.ch/demo/dropanalysis> [Accessed 18 January 2016].

STALDER, A. F., KULIK, G., SAGE, D., BARBIERI, L. & HOFFMANN, P. 2006. A snake-based approach to accurate determination of both contact points and contact angles.

Colloids and Surfaces a-Physicochemical and Engineering Aspects, 286, 92-103.

STALDER, A. F., MELCHIOR, T., MÜLLER, M., SAGE, D., BLU, T. & UNSER, M.

2010. Low-bond axisymmetric drop shape analysis for surface tension and contact angle

measurements of sessile drops. Colloids and Surfaces A: Physicochemical and

Engineering Aspects, 364, 72-81.

TAPPI 2000. Test Method T1200 sp-00 Interlaboratory evaluation of test methods to determine TAPPI repeatability and reproducibility. Atlanta, GA, USA: TAPPI Press.

VALAT, B., JOUANY, C. & RIVIERE, L. M. 1991. CHARACTERIZATION OF THE

WETTING PROPERTIES OF AIR-DRIED PEATS AND COMPOSTS. Soil Science,

152, 100-107.

VARGAFTIK, N., VOLKOV, B. & VOLJAK, L. 1983. International tables of the surface

tension of water. Journal of Physical and Chemical Reference Data, 12, 817-820.

WIJewardana, N. S., Kawamoto, K., Moldrup, P., Komatsu, T., Kurukulasuriya, L. C. & Priyankara, N. H. 2015. Characterization of water repellency for hydrophobized grains with different geometries and sizes. *Environmental Earth Sciences*, 74, 5525-5539.

Woodward, R. P. 1999. Contact angle measurements using the drop shape method. First Ten Angstroms Inc., Portsmouth, VA.

LIST OF FIGURE CAPTIONS

Figure 1. Schematic representation of contact angle measurement using the SDM

Figure 2. Evaluation of the surface tension of water using the pendant drop method

Figure 3. Variation of fit error (μm) with Relative Sharpness Index (RSI) (The values next to the data points are the respective surface tension values)

Figure 4. Ambiguity in identifying the baseline on granular materials

Figure 5. Variation of band thickness, B (mm) with particle size (mm)

Figure 6. Evaluation of techniques at different range of contact angles on flat and granular materials

Figure 7. Fitting of the drop profile by the *Tangent-2* method

Figure 8. Analysis of automated techniques by means of fit error (μm) on flat and granular materials

Figure 9. Steps in the measurement of contact angle (CA) on granular materials with proposed method. Step 1: Obtain image from goniometer after adjusting Relative Sharpness Index (RSI) to ≥ 70 . Step 2: Fitting of drop profile by Low-Bond Axisymmetric Drop Shape Analysis (LBADSA) method as per the recommendations of Stalder *et al.* (2010). Step 3: Binarisation of the image. Step 4: Generation of outlines of drop and surface. Step 5: Positioning the baseline as a horizontal tangent to the outline when moving upwards towards drop profile

Figure 10. Comparison of standard deviations amongst the techniques of measurement

Table 1. Standard deviations (maximum) of contact angles reported in literature

Referenced Article	Maximum standard deviation (corrected to 2 s.f)	Material
Bachmann <i>et al.</i>, 2000b	± 13	Gleyic Podzol (FAO Classification) – Fine to medium sand
Bachmann <i>et al.</i>, 2013	± 13	Gleyic Podzol (FAO Classification) – Sandy soil
Beatty & Smith, 2010	± 17	Organic soils from post wild-fire - Sandy soil
Goebel <i>et al.</i>, 2011	± 12	Gleyic Podzol (FAO Classification)
Koc & Bulut., 2014	± 6	Limestone
Leelamanie & Karube, 2012	± 6	Silica sand
Lourenço <i>et al.</i>, 2015a	± 25	Mixture of sand and clay
Wijewardana <i>et al.</i>, 2015	$\pm 15^\dagger$	Glass beads, Toyoura sand, Narita sand (Fine to medium fine)

[†] Average standard deviation reported

Table 2: Description of fitting methods for evaluation of contact angles (Source: KRÜSS GmbH, 2014)

Fitting Method	Description
Tangent-1	<p>An elliptical arc (a type of conic section) in the form: $Ax^2 + Cy^2 + Dx + Ey + F = 0$ is used to fit the drop profile by the least square algorithm. The CA is then obtained by determining the first derivative of the polynomial. With the <i>Tangent-1</i>, the polynomial is used to fit the whole drop profile yielding a single value of CA.</p>
Tangent-2	<p>The value of the CA is determined independently on each side of the drop profile at the three phase contact line by making use of an equation of the form $y = A + Bx + Cx^{0.5} + D/\ln x + E/x^2$. Unlike the <i>Tangent-1</i>, <i>Tangent-2</i> does not fit the whole drop profile and also gives two</p>

	<p>values of CAs on either side of the drop from which an average is usually calculated.</p>
Circle	<p>In this method, a circular arc is generated to the whole outline of the drop and the CA is obtained by fitting with the equation of the circle. In this case, as with <i>Tangent-1</i>, a single value of CA is obtained.</p>
Laplace-Young	<p>The <i>Laplace-Young</i> defines the CA by taking into consideration the gravitational and interfacial forces acting on the whole drop profile. The fitting makes use of the Young-Laplace equation (Eq. (1)), which relates the pressure difference across a curved surface (ΔP) to the surface tension (γ) and the</p>

curvature of the interface (r). An important assumption carried out in this fitting process is that the drop profile is considered axisymmetric, therefore giving only a single value of CA.

$$\Delta P = \frac{2\gamma}{r}$$

Eq. (1)

Table 3. Sensitivity of contact angles to the movement of the baseline on a microscope slide and on a hydrophobised microscope slide (Underlined values represent contact angles of hydrophobised microscope slide)

Automated Technique	Baseline Location		
	<i>At mirror image</i>	<i>0.1 mm below mirror image</i>	<i>0.1 mm above mirror image</i>
<i>Tangent-1</i>	34.7°	55.0°	26.7°
	<u>101.5°</u>	<u>98.7°</u>	<u>96.8°</u>
<i>Tangent-2</i>	28.1°	32.0°	22.8°
	<u>95.4°</u>	<u>56.1°</u>	<u>87.5°</u>
<i>Circle</i>	24.3°	27.1°	26.5°
	<u>92.7°</u>	<u>94.0°</u>	<u>88.3°</u>
<i>Laplace-Young</i>	29.8°	35.5°	32.8°
	<u>132.6°</u>	<u>98.7°</u>	<u>123.0°</u>

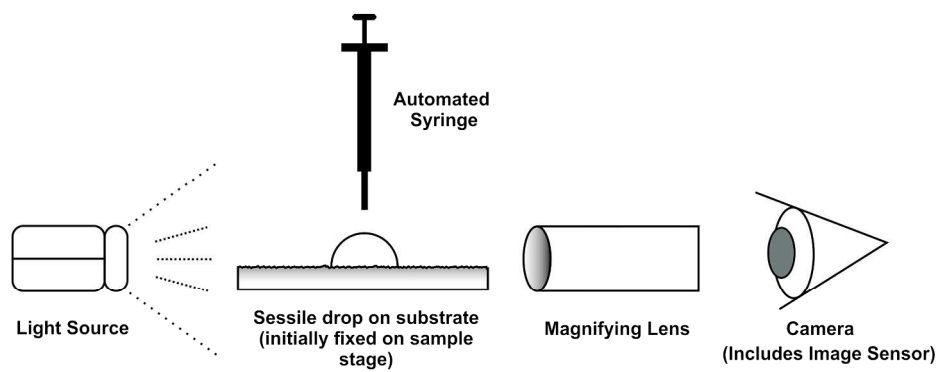


Figure 1. Schematic representation of contact angle measurement using the SDM

230x123mm (300 x 300 DPI)

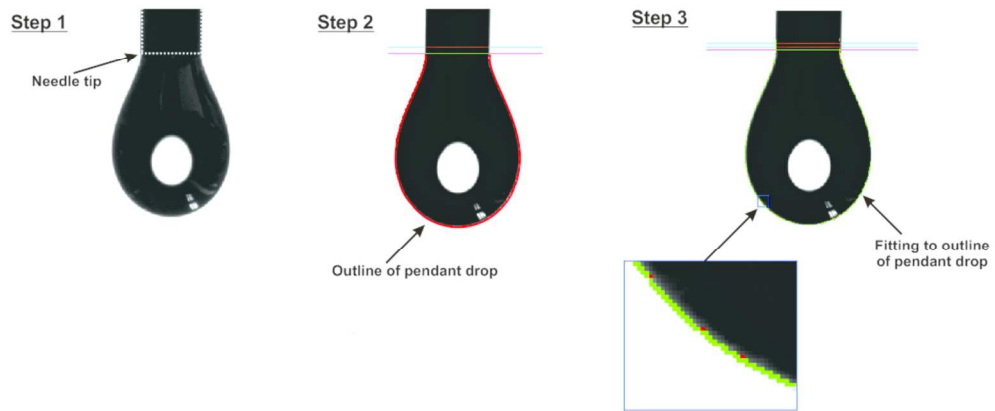


Figure 2. Evaluation of the surface tension of water using the pendant drop method

145x69mm (300 x 300 DPI)

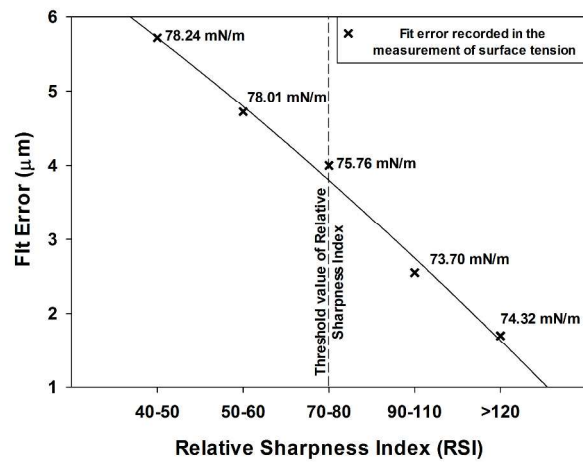


Figure 3. Variation of fit error (μm) with Relative Sharpness Index (RSI) (The values next to the data points are the respective surface tension values)

279x395mm (300 x 300 DPI)

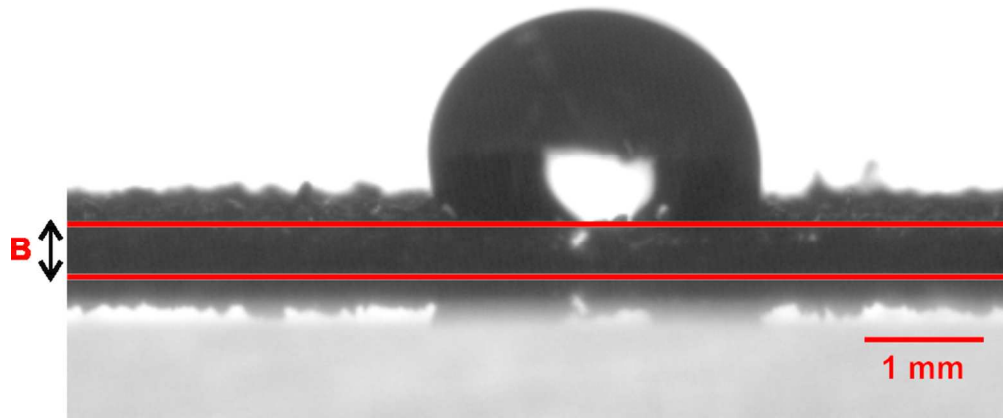


Figure 4. Ambiguity in identifying the baseline on granular materials

88x38mm (300 x 300 DPI)

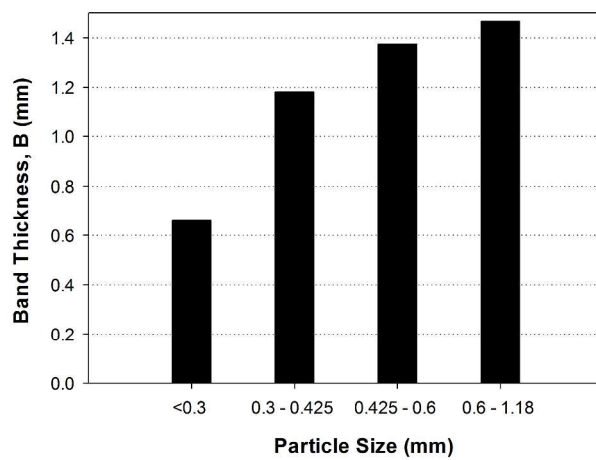


Figure 5. Variation of band thickness, B (mm) with particle size (mm)

279x395mm (300 x 300 DPI)

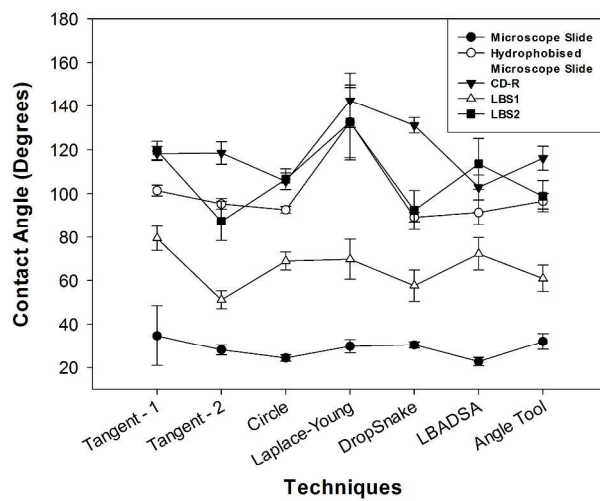


Figure 6. Evaluation of techniques at different range of contact angles on flat and granular materials

279x395mm (300 x 300 DPI)

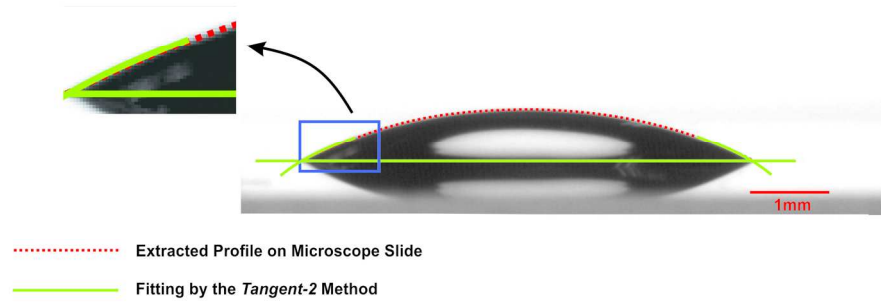


Figure 7. Fitting of the drop profile by the Tangent-2 method

177x85mm (300 x 300 DPI)

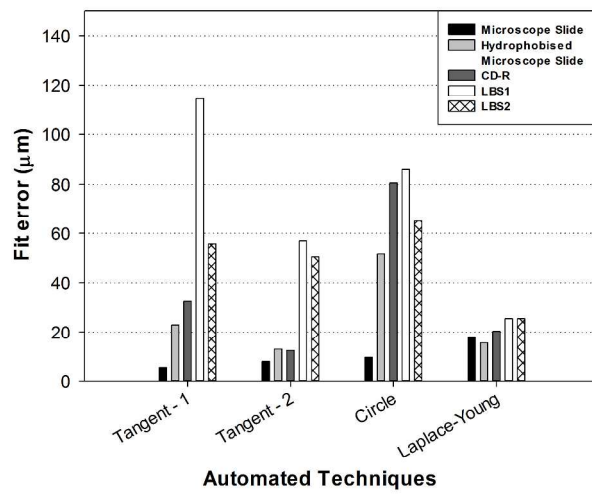


Figure 8. Analysis of automated techniques by means of fit error (μm) on flat and granular materials

279x395mm (300 x 300 DPI)

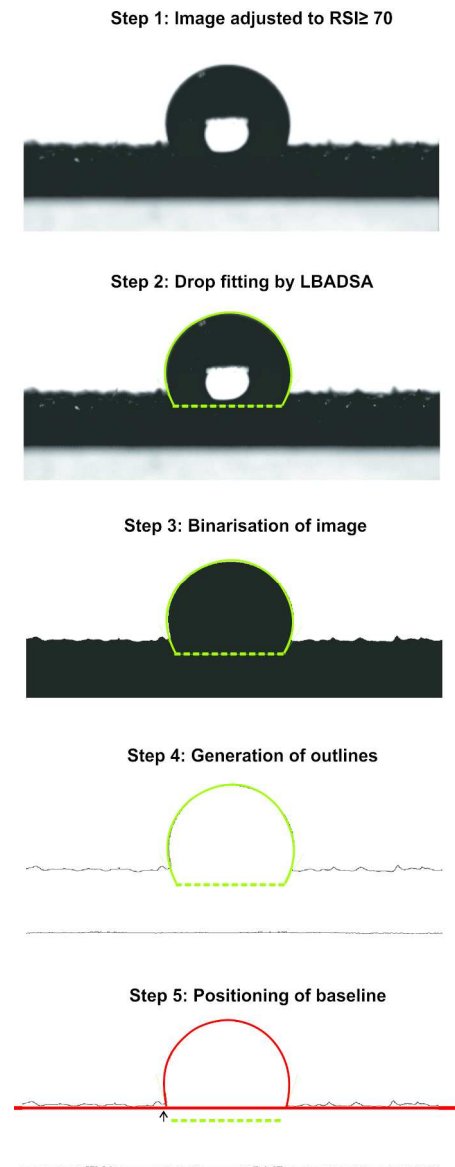


Figure 9. Steps in the measurement of contact angle (CA) on granular materials with proposed method. Step 1: Obtain image from goniometer after adjusting Relative Sharpness Index (RSI) to ≥ 70 . Step 2: Fitting of drop profile by Low-Bond Axisymmetric Drop Shape Analysis (LBADSA) method as per the recommendations of Stalder et al. (2010). Step 3: Binarisation of the image. Step 4: Generation of outlines of drop and surface. Step 5: Positioning the baseline as a horizontal tangent to the outline when moving upwards towards drop profile

108x288mm (300 x 300 DPI)

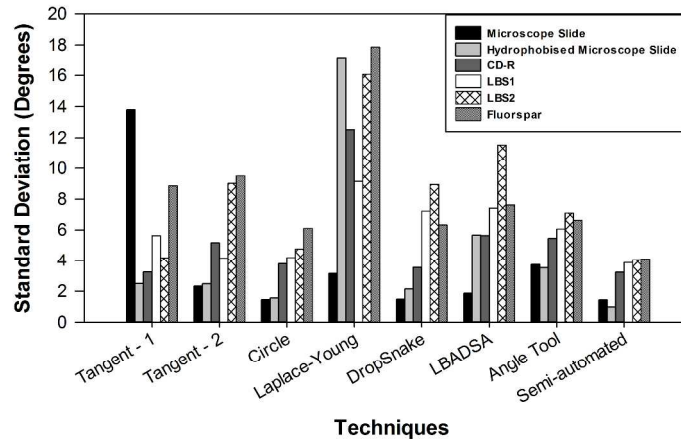


Figure 10. Comparison of standard deviations amongst the techniques of measurement

396x279mm (300 x 300 DPI)